Original Paper

Hollow glass microspheres/silicone rubber composite materials toward materials for high performance deep in-situ temperature-preserved coring

Jian-Ping Yang [a, b], Ling Chen [c, *], Xiao-Bin Gu [d], Zhi-Yu Zhao [e], Cheng-Hang Fu [f], Dong-Sheng Yang [a], Dong-Zhuang Tian [g], Zhi-Sheng Chen [g], He-Ping Xie [a, b]

[a] College of Polymer Science and Engineering, Sichuan University, Chengdu, 610065, China
[b] Guangdong Provincial Key Laboratory of Deep Earth Sciences and Geothermal Energy Exploitation and Utilization, Institute of Deep Earth Sciences and Green Energy, College of Civil and Transportation Engineering, Shenzhen University, Shenzhen, 518060, China
[c] School of Mechanical Engineering, Sichuan University, Chengdu, 610065, China
[d] Jinshi Drilltech Company Limited, Tangshan, 063004, Hebei
[e] Institute of New Energy and Low-Carbon Technology, Sichuan University, Chengdu, 610065, China
[f] College of Water Resource & Hydropower, Sichuan University, Chengdu, 610065, China
[g] Xi'an Research Institute, China Coal Technology & Engineering Group Corp, Xi'an, 710077, China

ARTICLE INFO

ABSTRACT

Deep petroleum resources are stored under high temperature and pressure conditions, with the temperature having a significant influence on the properties of rocks. Deep in-situ temperature-preserved coring (ITP-coring) devices were developed to assess deep petroleum reserves accurately. Herein, hollow glass microspheres (HGMs)/silicone rubber (SR) composites that exhibit excellent thermal insulation properties were prepared as thermal insulation materials for deep ITP-coring devices. The mechanism and process of heat transfer in the composites were explored, as well as their other properties. The results show that the HGMs exhibit good compatibility with the SR matrix. When the volume fraction of the HGMs is increased to 50%, the density of the HGMs/SR composites is reduced from 0.97 to 0.56 g/cm^3. The HGMs filler introduces large voids into the composites, reducing their thermal conductivity to 0.11 W/m·K. The addition of HGMs into the composites further enhances the thermal stability of the SR, wherein the higher the HGMs filler content, the better the thermal stability of the composites. HGMs significantly enhance the mechanical strength of the SR. HGMs increase the compressive strength of the composites by 828% and the tensile strength by 164%. Overall, HGMs improve the thermal insulation, pressure resistance, and thermal stability of HGMs/SR composites.

© 2021 The Authors. Publishing services by Elsevier B.V. on behalf of KeAi Communications Co. Ltd. This is an open access article under the CC BY license (http://creativecommons.org/licenses/by/4.0/).

1. Introduction

Natural resources have been gradually exhausted, with the depth at which the materials are located increasing year on year (Xie et al. 2015, 2019; Gao et al., 2018). For example, the depth for mining coal has reached 1500 m, the geothermal mining depth is > 3000 m, the ferrous metal mining depth is > 4350 m, and the depth required to drill for oil is >7500 m (Gao et al., 2021b; Xie et al., 2015b; Xie, 2017). Deep in-situ rocks experience three high types of "high conditions"; high temperature, high osmotic pressure, and high in-situ stress (Gao et al., 2020a). Among these, temperature significantly affects the physical and mechanical properties of rocks, as well as their permeability (Liang et al., 2005; Chen et al., 2019; Gao et al., 2021c). The rock cores obtained via common coring technology without preservation of their temperature seriously affect the accuracy of assessing petroleum resources (Pang et al., 2015; Gao et al., 2020b; Saif et al., 2017). Exploring the mechanism of deep in-situ temperature-preserved coring (ITP-coring) and developing deep ITP-coring devices are thus of great significance in assessing deep petroleum resources (Xie HP et al., 2020; Xie et al., 2021; Gao et al., 2021).

There have been many research studies on the temperature-preserved coring technology of natural gas hydrate. These studies have included a thermal insulation and pressure temperature core

* Corresponding author.
E-mail address: chenlingscu@scu.edu.cn (L. Chen).

List of symbols

K_g	the heat transfer coefficient of the gas in HGMs/SR composites, $W/m^2 \cdot K$
$K_{g,0}$	the initial heat transfer coefficient of the gas in HGMs, $W/m^2 \cdot K$
K_{SR}	the heat transfer coefficient of SR in HGMs/SR composites, $W/m^2 \cdot K$
$K_{SR,0}$	the initial heat transfer coefficient of SR, $W/m^2 \cdot K$
C_{SR}	the volume specific heat capacity of SR, $J/m^3 \cdot K$
v_{SR}	the average root mean velocity of SR phonons, m/s
d	the diameter of the HGMs, m

Greek letters

Π	the volume ratio of the HGMs cavity to the HGMs/SR composites, dimensionless
β	the parameter that represent the collision between the gas molecules in the HGMs and the inner surface of the HGMs, dimensionless
Λ_g	the free path of the gas molecules, m
Λ_{SR}	the average free path of SR phonons, m
δ	the minimum distance between the adjacent HGMs, m
η	the volume fraction of the HGMs, %
ρ_1	the density of the SR, kg/m^3
ρ_2	the density of the HGMs, kg/m^3

sampler (PTCS) developed in Japan (Kawasaki M, et al., 2006), a deep-water shallow hole thermal insulation and pressure-maintaining coring tool for natural gas hydrate developed by the first Institute of Oceanography of China (Zhang et al., 2006), a pressure and temperature preservation (PTP) system for natural gas hydrate developed by Zhu et al. (2013) and Milkov et al. (2004), and a multiple autoclave corer (MAC) and dynamic autoclave piston corer (DAPC) (Bohrmann et al., 2007; Heeschen et al., 2007). However, these temperature-preserved coring devices are used to keep natural gas hydrate at low temperatures (Pang et al., 2021), which is the opposite to ITP-coring devices, which are used to keep deep rock at high temperature. The thermal insulation methods used in temperature-preserved coring, including semiconductor Peltier chip refrigeration and liquid nitrogen refrigeration, thus cannot be used in ITP-coring. In addition, both the fidelity coring devices of the first Institute of Oceanology in China and PTPs (Dell'Agli et al., 2000; Di et al., 2010) involve the addition of an interlayer for thermal insulation, which leads to a decrease in the impact strength of coring devices and an increase in their size, which is associated with huge financial costs.

General thermal insulation materials are divided into organic thermal insulation materials and inorganic thermal insulation materials. Many inorganic materials, including thermal insulation coatings, have loose and porous structures and are not suitable for deep water-bearing environments. Organic insulation material is mostly plastic foam. Plastic foams will decompose thermally under high-temperature condition. Moreover, the plastic foam will absorb water in the high-pressure water, which results in loss of its thermal insulation performance. ZrO_2-8 %Y_2O_3 is coated on the outer surface of the outer pipe in the pressure and temperature preservation system for gas hydrate bearing developed by Zhu et al. (2013). Zhu et al. (2011) proposed polyurethane foam material as insulation material in pressure and temperature preservation techniques for gas hydrate-bearing sediments sampling. The thermal conductivity of ZrO_2-8% Y_2O_3 coating is relatively high, which is

1~2W/m·K. Polyurethane foam has many interconnected pores inside, which are easy to absorb water in long-term water environment. And polyurethane foams decompose at a high temperature of 150 °C. Polyurethane foam has poor elasticity and is easy to be destroyed under the disturbance of corer operation.

Therefore, there is a lack of thermal insulation materials that exhibit high pressure and temperature resistance in deep ITP-coring devices, limiting the development of coring devices and the accurate assessment of petroleum. To preserve the temperature of the in-situ core, coring devices must feature a thermal insulation material that is suitable for use under deep, high-temperature and high-pressure conditions. Polymer materials have long molecular chains and irregular amorphous structures, making them poor heat conductors that do not conduct phonons. Silicone rubber (SR) is a type of polymer material that exhibits stable chemical properties, as well as both low- and high-temperature resistance (Zhang et al., 2020; Ouyang et al., 2021). In addition, it is corrosion-resistant, and does not readily deteriorate. Moreover, it exhibits low thermal conductivity (Gao et al., 2013). Therefore, SR is suitable for use in deep ITP-coring devices. Hollow glass microspheres (HGMs) are microspheres that exhibit a hollow structure, which endows them with low thermal conductivity properties. Their micron size is convenient for adjusting the porosity of polymer materials, which can further reduce their thermal conductivity. Hollow glass microspheres/silicone rubber (HGMs/SR) is a composite material manufactured by compositing HGMs and SR (Zhao et al., 2021). Its structure is with tiny closed bubbles dispersed in the matrix. Herein, different HGMs were combined with SR to produce HGMs/SR composites that exhibit comprehensive thermal insulation and pressure resistance performance.

2. Theoretical analysis of the heat transfer in the HGMs/SR composites

2.1. Heat transfer of the gas phase HGMs/SR composites

In HGMs/SR composites, the gas phase is completely composed of the gas in the HGMs. According to the application conditions of ITP-coring devices, the heat transfer mechanism can be mainly divided into the following two parts.

(1) Thermal convection of gas in HGMs

According to the heat transfer equation of gas convection, only when the Grashof number is > 1000 can gas convection heat transfer occur. In the Grashof number equation, the heat conduction caused by gas convection is considered (Vedula et al., 1998) only when the size of the HGMs is larger than 10 mm. The diameter of the HGMs used to prepare thermal insulation materials in this experiment is far less than 10 mm, meaning that the effect that gas heat convection has on the heat conduction in the HGMs can be ignored.

(2) Heat conduction of gas in the HGMs

The gas heat conduction in the HGMs/SR composites mainly occurs due to the collision between air molecules in the HGMs and the collision between air molecules and the walls of the HGMs (Schiffres et al., 2012). According to the intrinsic thermal conductivity of gas and the structure of composite materials, K_g can be expressed using Eq. (1) (Lu et al. 1992, 1995; Zhao et al., 2012):

$$K_g = \frac{K_{g,0} \cdot \Pi}{1 + 2 \cdot \beta \cdot \Lambda_g / d} \tag{1}$$

It can be seen from Eq. (1) that increasing the average free path of the gas molecules in the cavity Λ_g or decreasing the cavity size of the HGMs d can reduce the heat transfer coefficient of the gas K_g.

2.2. Heat transfer of the SR in the HGMs/SR composites

The heat transfer of SR mainly occurs via the vibration of its molecules, where the minimum units of the vibrational energy are phonons. Therefore, the transmission properties of phonons in SR determine the heat transfer coefficient of the material. Combining the dynamic model (Chen, 2005) and the solid heat transfer coefficient equation, K_s, the contribution that SR makes toward the heat transfer coefficient of the HGMs/SR composites, can be expressed according to Eq. (2) (Hu et al., 2019):

$$K_{SR} = (1 - \Pi) \cdot K_{SR,0} = (1 - \Pi) \cdot \frac{1}{3} \cdot C_{SR,0} \cdot v_{SR} \cdot \left(\frac{1}{\Lambda_{SR}} + \frac{2}{d + \delta} \right)^{-1} \tag{2}$$

According to Eq. (2), when the cavity size of the HGMs d is much larger than the phonon-free path Λ_{SR}, the heat transfer mechanism of the HGMs/SR composites remains unchanged.

2.3. Analysis of the heat flow transfer of the HGMs/SR composites

According to Eqs. (1) and (2), increasing the porosity and reducing the cavity size can simultaneously reduce the heat transfer coefficient of the gas and solid phases in the HGMs, which endows the HGMs/SR composites with better thermal insulation properties. According to the filling conditions of the HGMs, the structures of the HGMs/SR composites can be simplified into five forms, as shown in Fig. 1, in which the blue part represents the SR matrix and the white part represents the HGMs. I corresponds to pure SR; II, III, and IV represent HGMs/SR composites filled with different amounts of HGMs; and V represents an HGMs/SR composites filled with too many HGMs, which results in them being crushed and destroyed.

According to Eqs. (1) and (2), the larger the volume fraction of the HGMs, the larger the porosity of the composites, and the lower the heat transfer coefficient, the better the thermal insulation properties of the HGMs/SR composites. The heat transfer of the HGMs/SR composites is schematically depicted in Fig. 2, in which the red lines represent the heat flow. For composite I, the heat flux flows smoothly through it, with its heat transfer coefficient being the highest, as the heat transfer coefficient of SR is higher than that of the HGMs. For the II, III, and IV composites, their thermal

insulation capacities are better than that of composite I. As the filling of the HGMs leads to an increase in porosity, the transfer of the heat flux in the composites is hindered to some extent. In composite V, the broken HGMs lead to the formation of additional thermal conduction pathways (Hu et al., 2013). The wall material of the HGMs is mainly silica, and its intrinsic thermal conductivity (1.34 W/m·K) is higher than that of the SR (0.19 W/m·K). Therefore, the heat conduction path formed by the broken HGMs is more conducive to heat flow propagation than that of the SR. Therefore, it is necessary to reasonably control the HGMs content to form the composite that has structure IV, to prepare HGMs/SR composites that exhibit the best thermal insulation properties.

3. Experimental methods

3.1. Materials

Silicon rubber prepolymer with a viscosity of 20000 cp, was purchased from the China Bluestar Research Institute. Different types of HGMs were purchased from 3M (the United States). The curing agent methyltris (methylethylketoxime) silane was purchased from Adamas-beta (Shanghai, China).

(1) SR

SR is a synthetic rubber that has a silicon−oxygen (Si−O) bonded the main chain and exhibits the characteristics of both an inorganic material and organic polymer (Kaewsikoun et al., 2020). For example, it is like an inorganic material in that it does not support combustion, and like an organic polymer, in the way that it exhibits low thermal conductivity. The Si−O bonds are ionic, with some of them in the form of double bonds, meaning that the actual length of the Si−O bonds is less than the theoretical value. The actual bond energy is also less than that of the theoretical value, and the Si−O bond energy of 460.5 kJ/mol is higher than those of the C−O bond energy of 358 kJ/mol and the C−C bond energy of 304 kJ/mol. Therefore, the thermal stability of SR is higher than that of general polymer materials. As the methyl group in SR can rotate freely around the Si−O bond, the SR molecular chain exhibits strong mobility and high flexibility, resulting in the glass transition temperature, T_g, of SR being low (Shit et al., 2013).

Due to its Si−O bonds, SR can be used over a wide temperature range (Zhao et al., 2015), exhibits good weather and aging resistance, and has special inert surface properties and chemical reaction inertia (Ghanbari-Slahkali et al., 2005). SR is suitable for the
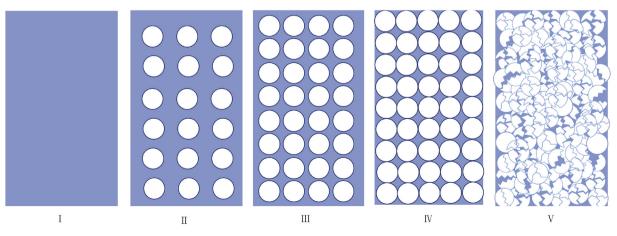

Fig. 1. Schematic of structures of the HGMs/SR composites.
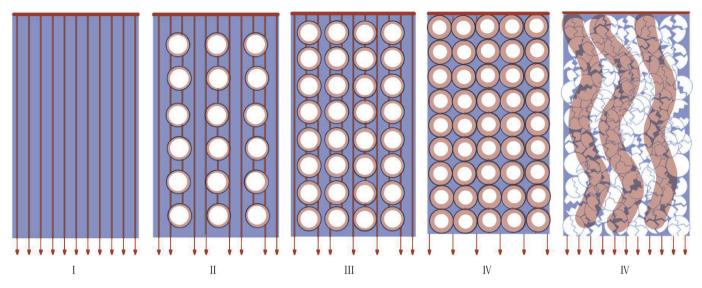
| I | II | III | IV | IV |

Fig. 2. Schematic of the heat transfer model of the HGMs/SR composites, in which the red lines represent the heat flow rate. In the case of the same heat transfer into the material, the less the heat flow, the better the insulation effect of the HGMs/SR composites.

preparation of a deep ITP-coring device due to its properties and usability under the deep environmental conditions of high temperature and pressure.

The SR used in this paper is hydroxyl-terminated polydimethylsiloxane, the structure of which is shown in Fig. 3, where R is alkyl side groups.

(2) HGMs

HGMs have a smooth surface and a simple structure which are shown in Fig. 4. The composition and surface properties of different types of HGMs are basically the same, but the main differences are the diameter and the wall thickness of HGMs. Their most typical structural feature is that they have a large cavity volume, which can be filled with air or inert gas. Due to the hollow structure of HGMs, they exhibit excellent properties, such as low thermal conductivity and density (Wu et al., 2021).

The properties of HGMs are shown in Table 1, in which the thermal insulation performance can be seen to be negatively correlated with the compressive strength. Of the compressive strength of the HGMs, that of the IM30K HGMs is the highest, but its thermal insulation performance is the worst. In contrast, the
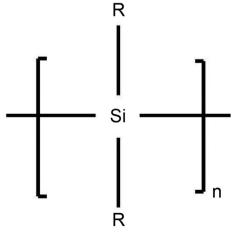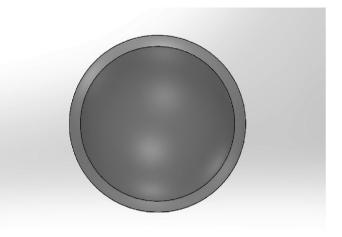

Fig. 4. The Schematic diagram of HGMs.

compressive strength of the K1 HGMs is the worst, but its thermal insulation performance is the best. These properties are related to particle size. The wall thickness of HGMs with large particle size is relatively thin, therefore meaning that the cavity structure is large. The main path of heat transfer is the air, which has very low thermal conductivity. Therefore, the heat preservation effect of the K1 HGMs is the best. Besides this, the larger the particle size, the smaller the critical stress that breaks K1 HGMs, thus making the compressive strength the lowest.

Since the compression performance of HGMs is negatively correlated with the thermal insulation performance, it is necessary to use different kinds of HGMs to compound with SR. The composite materials with excellent comprehensive properties of thermal insulation and compressive properties are obtained in this way.

3.2. Preparation of the HGMs/SR composites

HGMs/SR composites with stable chemical properties were prepared via a facile synthesis by combining HGMs with SR to give materials that exhibit good strength and excellent thermal insulation properties. Each type of HGMs was combined with SR to

Fig. 3. The structure of SR.

Table 1
Properties of different HGMs.

Type	Compressive strength,	Thermal conductivity,	Density,	Particle diameter distribution, um		
	MPa	W/m·K	g/cm³	10th%	50th%	90th%
K1	1.72	0.047	0.125	30	65	110
K25	5.17	0.085	0.250	25	55	95
K46	41.34	0.153	0.460	15	40	75
IM30K	192.92	0.200	0.600	9	16	25

prepare composites with around 10%, 20%, 30%, 40%, and 50% HGMs by volume fraction. Then, the composites with the best thermal insulation and mechanical properties were selected.

The specific preparation process of the HGMs/SR composites was as follows. SR, curing agent, catalyst, and HGMs were weighed into the relevant proportions and placed in a beaker. This beaker was then put into a defoaming vacuum mixer under a low shear force and stirred for three cycles (the parameters per cycle were stirring for 1.5 min at a rotation speed of 1800 rpm under a vacuum of 0.5 KPa). Damage to the HGMs was avoided as far as possible while still achieving homogeneous mixing. After efficient mixing and stirring, the composites precursor was injected into a specially designed polytetrafluoroethylene (PTFE) mold. The shapes of the test samples were prepared according to Chinese national standards GB/T 1040. And their tensile strength, compressive strength, and thermal insulation properties were characterized. After curing at room temperature for 24 h, the composites were demolded.

3.3. Design of thermal insulation system structure

HGMs/SR composites is a viscous state that can flow before curing. So, HGMs/SR can be easily molded and machined in the ITP-coring device. The structure diagram of the insulation system is shown in Fig. 5. HGMs/SR composites are filled in the annulus between the core chamber and the core sleeve of the corer. In this way, the heat loss of the type core can be effectively blocked. HGMs/SR is not the direct stress-bearing structure in this design. Due to the high elasticity, HGMs/SR can maintain the integrity of the material structure and thermal insulation performance under the corer disturbance.

3.4. Characterization methods

Density: Composites with different types of HGMs in different volume fractions were measured using a Beijing Dezhi Innovative instruments and equipment limited solid density tester. At least three sets of tests were performed on each sample to ensure test accuracy.

SEM: Morphologies of cross-sections of the composite materials were observed by scanning electron microscope (SEM) using an Apreo S HiVoc model microscope produced by Thermo Fisher Scientific. Before carrying out any observations, the samples were brittle broken using liquid nitrogen to decrease the mobility of the molecular segments of the SR. In the SEM measurements, the original morphologies of the HGMs/SR composites were observed to a great extent.

Thermal insulation performance: The thermal conductivity of the composite materials was measured using a TPS7 model hot disk thermal conductivity tester produced by Sweden Hot Disk. In these measurements, the lower the thermal conductivity, the better the thermal insulation properties. Repeated tests were conducted in each group of samples to improve the accuracy and reliability of the test data.

Mechanical properties: Tensile and compressive strength measurements of the HGMs/SR composite materials were carried out using a 5967-model electronic pulling force instrument produced by Instron. Each group of samples was tested several times to ensure test accuracy.

4. Results and discussion

4.1. Density analysis

The density of the HGMs used in the experiment is lower than that of the SR. According to both theoretical predictions and actual measurements, the density of the composites decreases with an increase in the HGMs content. Neglecting the effect that the SR curing has on the volume shrinkage, the relationship between the HGMs/SR density and HGMs volume fraction can be expressed using the Eq. (3):

$$\rho = \rho_1 \cdot (1 - \eta) + \rho_2 \tag{3}$$

The results in Fig. 6 show that the measured density of the samples is lower than the theoretically predicted density, which is mainly due to the air mixed in the composites. With an increase in the volume fraction of the HGMs, the more air that is introduced in the mixing process, the greater the deviation of the measured density from the theoretical density. The overall trend is that the density of the samples decreases with an increase in the volume fraction of the HGMs. The density of the composites is directly
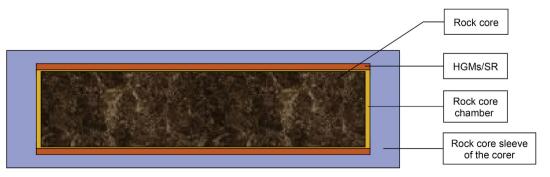

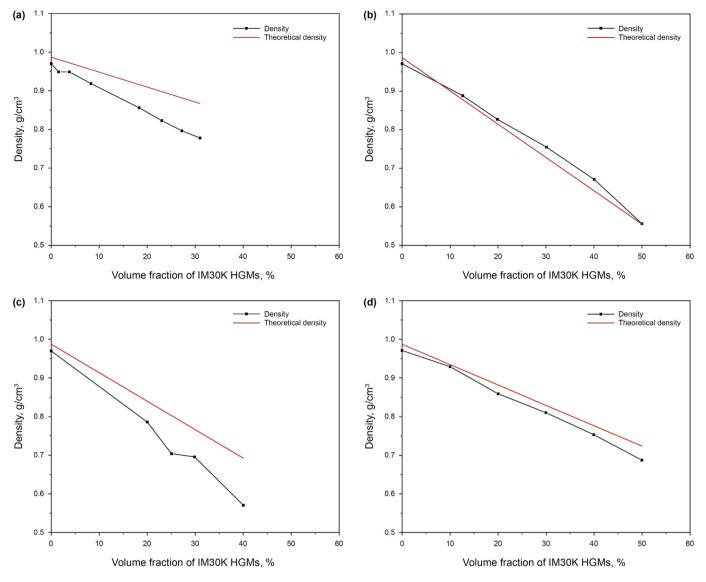**Fig. 5.** Schematic diagram of thermal insulation system structure.

Fig. 6. Relationship between the density of the composites and the volume fraction of the HGMs for the **a** IM30K, **b** K1, **c** K25, and **d** K46 HGMs/SR composites.

related to their thermal insulation properties. Generally speaking, the lower the density of the material, the lower the thermal conductivity of the composites, and the better their thermal insulation properties.

4.2. Morphological analysis

1) Morphological analysis of the HGMs

The morphologies and structures of the four types of HGMs were measured. Before measuring the HGMs, they were placed under a vacuum. If the HGMs contain air, the force will destroy their shells when they are placed under a vacuum. Fig. 7 shows SEM images of the broken shells of the HGMs, from which their hollow structures can be observed. From the images, it can be seen that the IM30K HGMs have the smallest particle size and experience the minimum damage, whereas the K series has the lowest strength and experience the most damage, with the K1 HGMs being the worst.

2) Morphological analysis of the HGMs/SR composites

Figs. 8−10 show SEM images of the HGMs/SR composites. Fig. 8a and b shows that there is good compatibility between the HGMs and the SR matrix. The HGMs circled with a red dotted line in Fig. 8b are almost immersed in the SR, and there is no obvious dividing line between them. The transition is quite natural, which indicates that the compatibility between the HGMs and SR is good. This is because of the large number of Si−O bonds in both the SR and the main components of the HGMs. Fig. 8c indicates that HGMs are fairly evenly distributed with the high-volume fraction of HGMs. The red dotted line in Fig. 8d shows that SR acts as an adhesive that bonds the HGMs. The red dotted line in Fig. 9a and c indicates obvious broken traces of the HGMs. From this image it can be observed that the shells of the HGMs are agglomerated, which indicates that the SR occupies the original voids of the broken HGMs. As the porosity of the HGMs/SR composites decreases, there is an increase in their thermal conductivity and a decrease in their thermal insulation properties. The degree of damage to the HGMs is directly related to their strength, and it can be seen from Fig. 9b and c that the K1 HGMs exhibits the lowest strength and most damage.

Fig. 10a shows that the distribution of the HGMs is stratified. Meanwhile, Fig. 10b shows that the dense hollow beads are
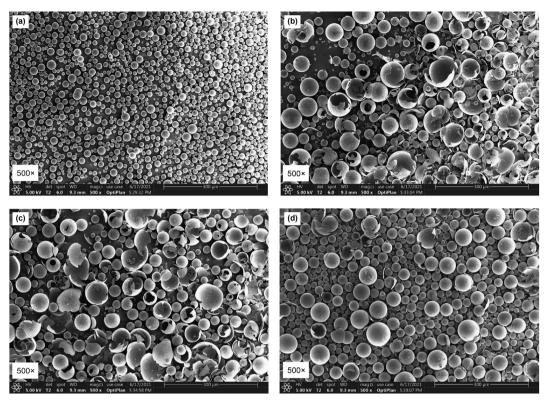
Fig. 7. SEM images of the HGMs for the **a** IM30K, **b** K1, **c** K25, and **d** K46 HGMs.

distributed above the dividing line in sharp contrast to the sparse ones below the dividing line. As the density of the HGMs is lower than that of the SR, in the process of material preparation, before the curing of the SR, the HGMs are buoyant on the surface of the SR. The uneven distribution of the HGMs directly affects the thermal conductivity and mechanical properties of the corresponding HGMs/SR composites. To solve the issues associated with the uneven distribution of the HGMs, in the future 1) the curing process can be improved to reduce the curing time; 2) a curing agent accelerator can be added to accelerate the curing process of the SR after the dispersion is uniform; and 3) the curing temperature of SR can be reduced as the viscosity of SR increases at low temperature, which hinders the buoyancy of the HGMs.

4.3. Analysis of thermal insulation properties of the HGMs/SR composites

Heat transfer coefficient reflects the ability of a substance to transfer heat by all means. Thermal conductivity reflects the ability of a substance to transfer heat by means of heat conduction (Zhao et al., 2018). According to the properties of HGMs/SR composites and its application environment, the main way of heat transfer of the composite materials is heat conduction. Therefore, thermal conductivity is used to characterize the thermal insulation performance of composite materials.

A series of samples with low thermal conductivity were prepared by varying the type and amount of the HGMs used as a filler. Fig. 11 shows the influence that the HGMs filling amount has on the composites. It can be seen from the data that the thermal conductivity of pure SR is 0.186 W/m·K, which is lower than those of metals and inorganic materials, showing that it is suitable to be used as the matrix material of a material with thermal insulation properties. The data in Fig. 11 also shows that the thermal

conductivity of the composites decrease with an increase in the volume fraction of the HGMs, for both the K series and IM30K HGMs/SR composites. In particular, when the filling volume fraction of the K1 HGMs is 50%, the thermal conductivity of the corresponding composites is the lowest, at 0.113 W/m·K. The thermal conductivity of the K46 HGMs/SR composites decreases before the volume fraction of the HGMs reaches 40%, but begins to rise when it increases to 50%. From this and the previous analysis on the morphology and heat transfer of the HGMs/SR composites, the reason for this is the overfilling of the HGMs, resulting in them crushing one another. In this scenario, a new heat conduction path is formed as in form (V) in the 2.3 analysis.

It is worth noting that the thermal conductivity of the IM30K, K1, and K25 HGMs/SR composites are similar up to a fill volume of 30 vol%, after which a slowly declining trend is observed. The thermal conductivity of the K25 HGMs/SR composites decreases rapidly. Nevertheless, the HGMs of the K25 HGMs/SR composites only can be filled by up to 40 vol%, due to the high viscosity of the SR. In addition, the thermal conductivity of the K25 and K1 HGMs/SR composites are close when the volume fraction of the HGMs is around 40%. The trend in the thermal conductivity of the K25 HGMs/SR composites gradually slows down, while that of the K1 HGMs/SR composites shows an obvious decrease. Therefore, it can be inferred that at a volume fraction of the K1 HGMs of 50%, the corresponding composites exhibits the lowest thermal conductivity and the best thermal insulation properties among the composites.

4.4. Analysis of the thermal stabilities of the HGMs/SR composites

The bond energy of the Si−O bonds that make up the main chain of SR is higher than that of carbon-based polymers, which means that SR exhibits higher thermal stability than carbon-based
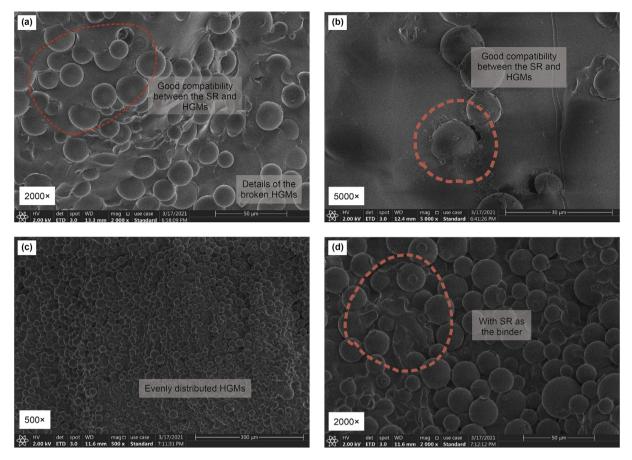
Fig. 8. a the IM30K HGMs/SR composites with 20 vol% of the IM30K HGMs; **b** the IM30K HGMs/SR composites with 4 vol % of the IM30K HGMs; **c** and **d** the IM30K HGMs/SR composites with 31 vol% of the HGMs.
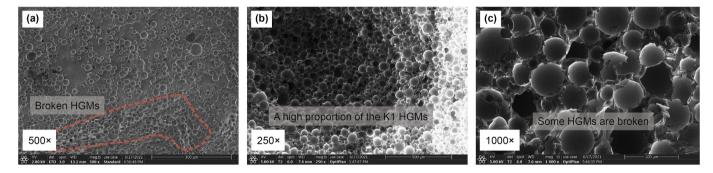

Fig. 9. a the IM30K HGMs/SR composites with 4 vol% of the IM30K HGMs; **b** and **c** the K1 HGMs/SR composites with 50 vol% of the K1 HGMs.

polymers. As can be seen in Fig. 12, the initial thermal decomposition temperature of pure SR is 389.2 °C. Moreover, there are two peaks, at 405.3 and 479.6 °C. The end temperature of the thermal decomposition is 505.2 °C. The results show that the thermal stabilities of the HGMs/SR composites are further enhanced after they are filled with the HGMs. The initial thermal decomposition temperature of the HGMs/SR composites becomes increasingly higher in line with an increase in the HGMs, which is 400.6 °C at 15 vol% of HGMs and 466.8 °C at 31 vol% of HGMs. The corresponding end temperatures of the thermal decomposition also become increasingly higher, at 564.1 °C at 15 vol% of HGMs and 563.2 °C at 31 vol% of HGMs.

The reasons for the high thermal decomposition temperatures of the composites are as follows. 1) HGMs are added into the SR, and the HGMs do not decompose in the temperature range used in the thermal analysis (25—800 °C). The thermal conductivity of the HGMs is lower than that of the SR. Therefore, under the same experimental conditions, a higher temperature is required to break the Si—O bonds. 2) The main component of the HGMs is SiO_2, which interacts with the Si—O bonds of the SR to make the composites more stable, therefore resulting in an increase in the thermal decomposition temperature.

4.5. Analysis of the mechanical properties of the HGMs/SR composites

The molecular chains of SR are flexible, resulting in it exhibiting a low glass T_g, being viscous at room temperature, and having
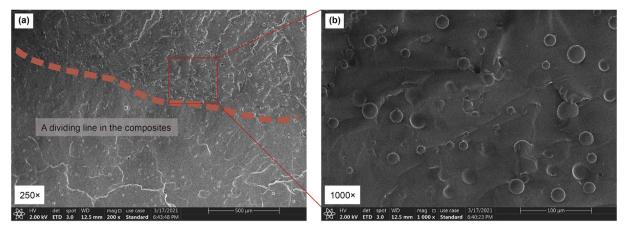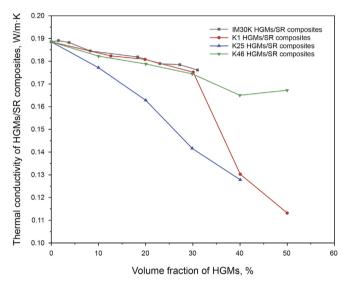
Fig. 10. **a** and **b** the IM30K HGMs/SR composites with 4 vol% of the IM30K HGMs.

Fig. 11. Influence of the type and filling amount of the HGMs on the thermal conductivities of the HGMs/SR composites.

elastic properties, a large recoverable elastic deformation, and poor mechanical properties. Fig. 13 shows the influence that the content and type of the HGMs have on the mechanical properties of the corresponding composites. From Fig. 13, it can be seen that the compressive and tensile strengths of the HGMs/SR composites increase in line with their hollow volume fractions. It is worth noting that the IM30K HGMs/SR composites have the highest strength and the K1 HGMs/SR composites the lowest. However, their values are quite close and far higher than those of pure SR. The increase in the tensile strength of the composites with the IM30K HGMs relative to SR is 164% and the increase in the compressive strength of the composites with the K46 HGMs relative to SR is 828%. The compressive and tensile strengths of the HGMs/SR composites are increased by 466% and 108%, respectively, at an HGMs filling volume of 50%. However, the compressive strengths of the composites are quite different from their hydrostatic compressive strengths. The main reason for this is that the strength of SR is low, and its deformation is large when under stress, which leads to its displacement and contact with the HGMs filler. When the HGMs are in contact with each other, the spherical structures of the HGMs lead to a concentration of stress, which results in their breakage.

4.6. Comparative analysis of the thermal insulation and pressure resistance of the HGMs/SR composites

Taking the K1 HGMs/SR composites as an example, the curves of their thermal conductivity and compressive strength according to the volume fraction of the HGMs are shown in Fig. 14. The data shows that an increase in the filling amount of the HGMs improves the compressive strength and reduces the thermal conductivity of the composites. In other words, the filled HGMs both improve the thermal insulation and the pressure resistance of the composites. This breaks the traditional concept that thermal conductivity and compressive strength tend to show opposite trends.

In terms of thermal insulation properties, the hollow structure is introduced into the composites upon the filling of the HGMs. This increases the closed porosity, preventing the propagation of heat flow in the composites, and therefore leading to an improvement in the thermal insulation properties of the composites. In terms of pressure resistance, the load-bearing phase of the composites changes from the former elastic SR to both HGMs and SR. The intrinsic compressive strength of the HGMs is greater than that of the SR, therefore leading to an improvement in the compressive strength of the composites.

According to the heat transfer analysis above and the experimental results, to simultaneously improve the thermal insulation properties and pressure resistance of the composites, it is necessary to increase their porosity and also increase the intrinsic strength of the matrix material. To improve the compressive strength of SR, which functions as the matrix material in the composites, its molecular structure should be modified. For example, rigid side groups can be introduced into the molecular chain of the SR, and its curing cross-linking nodes can be increased to increase its degree of curing.

5. Conclusions

To meet the needs of deep ITP-coring devices, composite materials were prepared with excellent thermal insulation properties by combining different types of HGMs with SR. The specific conclusions of this research are as follows.

The HGMs fillers enhance the thermal insulation and pressure resistance properties of the corresponding composites. Upon an increase in the volume fraction of the K1 HGMs from 0% to 50%, the thermal conductivity of the composites decreases from 0.19 to 0.11 W/m·K, and the compressive strength of the composites increases by 460%, from 0.065 to 0.37 MPa. This shows that the thermal insulation resistance and pressure resistance properties
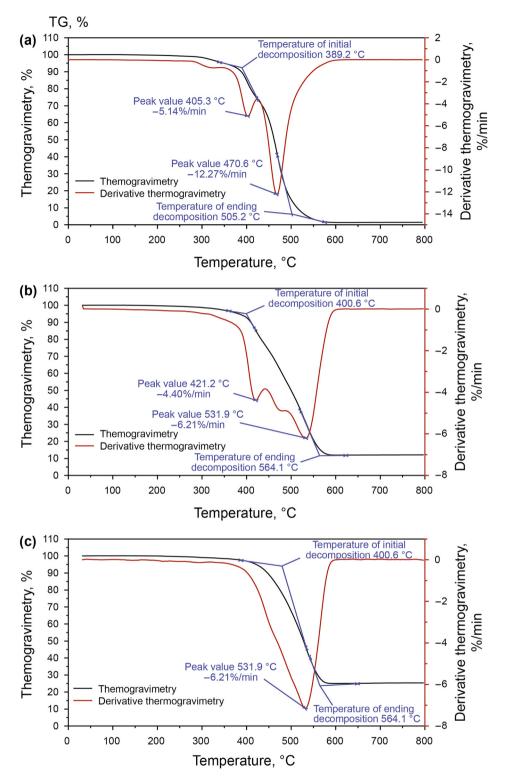
Fig. 12. Thermal analysis curves of SR and two HGMs/SR composites. **a** Pure SR. **b** HGMs/SR composites with 15 vol% IM30K HGMs. **c** HGMs/SR composites with 31 vol% IM30K HGMs.

can be simultaneously improved by introducing porosity and high strength bearing phase into the composites.

The HGMs/SR thermal insulation composites prepared in this work exhibit excellent thermal stability (a thermal decomposition temperature of up to 466.8 °C), as well as strong corrosion and weather resistance. The composite materials are intended to be used in deep ITP-coring devices, but they can also be used for thermal insulation of oil pipelines in transportation processes and thermal insulation of high-temperature pipelines in the chemical industry.

A disadvantage of the HGMs/SR thermal insulation composites prepared in this work is that their compressive strength is not high
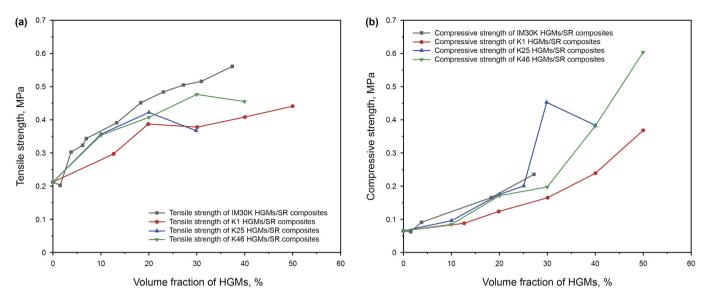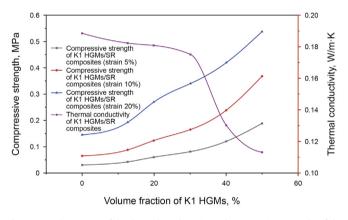
Fig. 13. a Tensile strengths (fracture strengths) of the HGMs/SR composites according to their volume fraction of HGMs. **b** Compressive strengths (compressive strain 10%) of the HGMs/SR composites according to the volume fraction of HGMs.

Fig. 14. Coupling curves of the thermal conductivity and compressive strengths of the K1 HGMs/SR composites.

enough. The highest compressive strength of the K46 HGMs/SR composites is only 0.60 MPa. Therefore, in future work, the molecular structure of SR will be further modified to improve the pressure resistance properties of the composites.

The thermal insulation and mechanical properties of the HGMs/SR composites developed in this work have been exploring in-depth under high temperature and pressure conditions. Overall, HGMs/SR composites have been designed and improved toward the development of materials for use in ITP-coring devices.

Declaration of competing interest

The authors declare that they have no conflicts of interest.

Acknowledgments

References

Bohrmann, G., Kuhs, W.F., Klapp, S.A., et al., 2007. Appearance and preservation of natural gas hydrate from Hydrate Ridge sampled during ODP Leg 204 drilling. Mar. Geol. 244 (1–4), 1–14. https://doi.org/10.1016/j.margeo.2007.05.003.

Chen, G., 2005. Nanoscale Energy Transport and Conversion: a Parallel Treatment of Electrons, Molecules, Phonons, and Photons. Oxford university press, New York, the United States.

Chen, L., Chu, Y.J., Zhang, Y., et al., 2019. Analysis of heat transfer characteristics of fractured surrounding rock in deep underground spaces. Math. Probl Eng. 2019. https://doi.org/10.1155/2019/1926728.

Dell'Agli, G., Mascolo, G., 2000. Low temperature hydrothermal synthesis of ZrO2-CaO solid solutions. J. Mater. Sci. 35 (3), 661–665. https://doi.org/10.1023/a:1004740830928.

Di, G., Blasi, C., Schioppa, M., et al., 2010. Structure and thermal properties of heat treated plasma sprayed ceria yttria co-stabilized zirconia coatings. Ceram. Int. 36 (3), 961–968. https://doi.org/10.1016/j.ceramint.2009.10.020.

Gao, J., Wang, J.B., Xu, H.Y., et al., 2013. Preparation and properties of hollow glass bead filled silicone rubber foams with low thermal conductivity. Mater. Des. 46, 491–496. https://doi.org/10.1016/j.matdes.2012.08.070.

Gao, M.Z., Xie, J., Gao, Y.N., et al., 2021a. Mechanical behavior of coal under different mining rates: a case study from laboratory experiments to field testing. Int. J. Min. Sci. Technol. 31 (5), 825–841. https://doi.org/10.1016/j.ijmst.2021.06.007.

Gao, M.Z., Xie, J., Guo, J., et al., 2021b. Fractal evolution and connectivity characteristics of mining-induced crack networks in coal masses at different depths. Geomechanics and Geophysics for Geo-Energy and Geo-Resources 7 (1), 1–15. https://doi.org/10.1007/s40948-020-00207-4.

Gao, Ming-Zhong, Chen, Ling, Fan, Dong, et al., 2021c. Principle and technology of coring with in-situ pressure and gas maintaining in deep coal mine. J. China Coal Soc. 46 (03), 885–897. https://doi.org/10.13225/j.cnki.jccs.YT21.0297 (in Chinese).

Gao, Ming-Zhong, Zhang, Jian-Guo, Li, Sheng-Wei, et al., 2020a. Calculating changes in fractal dimension of surface cracks to quantify how the dynamic loading rate affects rock failure in deep mining. J. Cent. S. Univ. 27 (10), 3013–3024. https://doi.org/10.1007/s11771-020-4525-5.

Gao, Ming-Zhong, Liu, Jun-Jun, Lin, Wen-Ming, et al., 2020b. Study on In-Situ Stress Evolution Law of Ultra - Thick Coal Seam in Advance Mining 48 (02), 28–35. https://doi.org/10.13199/j.cnki.cst.2020.02.003 (in Chinese).

Gao, M.Z., Zhang, R., Xie, J., et al., 2018. Field experiments on fracture evolution and correlations between connectivity and abutment pressure under top coal caving conditions. Int. J. Rock Mech. Min. Sci. 111, 84–93. https://doi.org/10.1016/j.ijrmms.2018.01.003.

Ghanbari-Slahkali, A., Mitra, S., Kingshott, P., et al., 2005. Investigation of the hydrothermal stability of cross-linked liquid silicone rubber (LSR). Polym. Degrad. Stabil. 90 (3), 471–480. https://doi.org/10.1016/j.polymdegradstab.2005.04.016.

Heeschen, K.U., Haeckel, M., Hohnberg, H.J., et al., 2007. Pressure coring at gas hydrate-bearing sites in the eastern Black Sea off Georgia. egu general assembly, 1 (40), 1–10.

Hu, F., Wu, S.Y., Sun, Y.G., 2019. Hollow-structured materials for thermal insulation. Adv. Mater. 31 (38). https://doi.org/10.1002/adma.201801001.

Hu, Y., Mei, R.G., An, Z.G., et al., 2013. Silicon rubber/hollow glass microsphere composites: influence of broken hollow glass microsphere on mechanical and thermal insulation property. Compos. Sci. Technol. 79, 64–69. https://doi.org/

10.1016/j.compscitech.2013.02.015.

Kawasaki, M., Umezu, S., Yasuda, M., 2006. Pressure temperature core sampler (PTCS). J. Jpn. Assoc. Pet. Technol. 71, 139–147. https://doi.org/10.3720/japt.71.139 (in Japanese).

Kaewsikoun, S., Kumarn, S., Sakdapipanich, J., 2020. The effect of non-rubber components on mechanical properties of TESPD silane coupling agent in silica-filled rubber compounds. IOP Conf. Ser. Mater. Sci. Eng. 773, 12–29. https://doi.org/10.1088/1757-899x/773/1/012029.

Liang, B., Gao, H.M., Lan, Y.W., 2005. Theoretical analysis and experimental study on relation between roack permeabikity and temperature. Chin. J. Rock Mech. Eng. 24 (12), 2009–2012. https://doi.org/10.3321/j.issn:1000-6915.2005.12.002 (in Chinese).

Lu, X., Caps, R., Fricke, J., et al., 1995. Correlation between structure and thermal conductivity of organic aerogels. J. Non-Cryst. Solids 188 (3), 226–234. https://doi.org/10.1016/0022-3093(95)00191-3.

Lu, X., Wang, P., Arduini-Schuster, M.C., et al., 1992. Thermal transport in organic and opacified silica monolithic aerogels. J. Non-Cryst. Solids 145 (1), 207–210. https://doi.org/10.1016/S0022-3093(05)80457-0.

Milkov, A.V., Dickens, G.R., Claypool, G.E., et al., 2004. Co-existence of gas hydrate, free gas, and brine within the regional gas hydrate stability zone at Hydrate Ridge (Oregon margin): evidence from prolonged degassing of a pressurized core. Earth Planet Sci. Lett. 222 (3–4), 829–843. https://doi.org/10.1016/j.epsl.2004.03.028.

Ouyang, Y., Li, X., Tian, H., et al., 2021. A Novel branched Al2O3/Silicon rubber composite with improved thermal conductivity and excellent electrical insulation performance. Nanomaterials 11 (10). https://doi.org/10.3390/nano11102654.

Pang, X.Q., Chen, Z.H., Jia, C.Z., et al., 2021. Evaluation and re-understanding of the global natural gas hydrate resources. Petrol. Sci. 18 (2), 323–338. https://doi.org/10.1007/s12182-021-00568-9.

Pang, X.Q., Jia, C.Z., Wang, W.Y., 2015. Petroleum geology features and research developments of hydrocarbon accumulation in deep petroliferous basins. Petrol. Sci. 12 (1), 1–53. https://doi.org/10.1007/s12182-015-0014-0.

Saif, T., Lin, Q.Y., Bijeljic, B., et al., 2017. Microstructural imaging and characterization of oil shale before and after pyrolysis. Fuel 197, 562–574. https://doi.org/10.1016/j.fuel.2017.02.030.

Schiffres, S.N., Kim, K.H., Hu, L., et al., 2012. Gas diffusion, energy transport, and thermal accommodation in single-walled carbon nanotube aerogels. Adv. Funct. Mater. 22 (24), 5251–5258. https://doi.org/10.1002/adfm.201201285.

Shit, S.C., Shah, P., 2013. A review on silicone rubber. Natl. Acad. Sci. Lett. 36 (4), 355–365. https://doi.org/10.1007/s40009-013-0150-2.

Vedula, V.R., Green, D.J., Hellmann, J.R., et al., 1998. Test methodology for the thermal shock characterization of ceramics. J. Mater. Sci. 33 (22), 5427–5432. https://doi.org/10.1023/a:1004410719754.

Wu, X.F., Gao, Y., Wang, Y., et al., 2021. Recent developments on epoxy-based

syntactic foams for deep sea exploration. J. Mater. Sci. 56 (3), 2037–2076. https://doi.org/10.1007/s10853-020-05420-w.

Xie, H.P., Gao, F., Ju, Y., 2015a. Research and development of rock mechanics in deep ground engineering. Chin. J. Rock Mech. Eng. 11 (34), 2162–2178. https://doi.org/10.13722/j.cnki.jrme.2015.1369 (in Chinese).

Xie, H.P., Gao, F., Ju, Y., et al., 2015b. Quantitative definition and investigation of deep mining. Mtan Xuebao/J. China Coal Soc. 40 (1), 1–10. https://doi.org/10.13225/j.cnki.jccs.2014.1690 (in Chinese).

Xie, H.P., Gao, M.Z., Zhang, R., et al., 2020. Study on concept and progress of in situ fidelity coring of deep rocks. Chin. J. Rock Mech. Eng. 39 (5), 865–876. https://doi.org/10.13722/j.cnki.jrme.2020.0138 (in Chinese).

Xie, H.P., Konietzky, H., Zhou, H.W., 2019. Special issue "deep mining.". Rock Mech. Rock Eng. 52 (5), 1415–1416. https://doi.org/10.1007/s00603-019-01805-9.

Xie, H.P., 2017. Research framework and anticipated results of deep rock mechanics and mining theory. Adv. Eng. Sci. 49 (2), 1–16. https://doi.org/10.15961/j.jsu-ese.201700025 (in Chinese).

Xie, He-Ping, Liu, Tao, Gao, Ming-Zhong, et al., 2021. Research on in-situ condition preserved coring and testing systems. Petrol. Sci. https://doi.org/10.1016/j.petsci.2021.11.003.

Zhang, Y., Jiang, Z., Yu, P., et al., 2006. NGH Deepwater Shallow Hole Heat Preservation and Pressure Holding Core Drilling Tool. China patent for invention CN1818323 (in Chinese).

Zhang, Y.L., Zang, C.G., Jiao, Q.J., et al., 2020. Heat-insulating materials with high-temperature resistance through binding hollow glass microspheres with vinyl-functionalized polyborosiloxane. J. Mater. Sci. 55 (29), 14264–14279. https://doi.org/10.1007/s10853-020-05046-y.

Zhao, C., Diao, S., Yuan, Y., et al., 2021. Preparation and properties of hollow glass microsphere/silicone rubber composite material with the transition layer of silicone resin. Silicon 13 (2), 517–522. https://doi.org/10.1007/s12633-020-00472-8.

Zhao, C.C., Zhang, J., 2015. Silicon Rubber and its Application. Chemical Industry Press, Beijing, China (in Chinese).

Zhao, J.J., Duan, Y.Y., Wang, X.D., et al., 2012. Effects of solid-gas coupling and pore and particle microstructures on the effective gaseous thermal conductivity in aerogels. J. Nanoparticle Res. 14 (8). https://doi.org/10.1007/s11051-012-1024-0.

Zhao, X.W., Zang, C.G., Sun, Y.L., et al., 2018. Effect of hybrid hollow microspheres on thermal insulation performance and mechanical properties of silicone rubber composites. J. Appl. Polym. Sci. 135 (11). https://doi.org/10.1002/app.46025.

Zhu, H.Y., Liu, Q.Y., Deng, J.G., et al., 2011. Pressure and temperature preservation techniques for gas-hydrate-bearing sediments sampling. Energy 36 (7), 4542–4551. https://doi.org/10.1016/j.energy.2011.03.053.

Zhu, H.Y., Liu, Q.Y., Wong, G.R., et al., 2013. A pressure and temperature preservation system for gas-hydrate-bearing sediments sampler. Petrol. Sci. Technol. 31 (6), 652–662. https://doi.org/10.1080/10916466.2010.531352.